


RESEARCH ARTICLE

Loss of myoepithelial calponin-1 characterizes high-risk ductal carcinoma in situ cases, which are further stratified by T cell composition

Elizabeth Mitchell¹ | Sonali Jindal^{1,2} | Tiffany Chan¹ | Jayasri Narasimhan¹ |
Shamilene Sivagnanam³ | Elliot Gray⁴ | Young Hwan Chang⁴ | Sheila Weinmann⁵ |
Pepper Schedin^{1,2} 

¹Department of Cell, Developmental, and Cancer Biology, Oregon Health and Science University, Portland, Oregon

²Cancer Prevention and Control, Knight Cancer Institute, Oregon Health and Science University, Portland, Oregon

³Computational Biology Program, Department of Cell, Developmental, and Cancer Biology, Oregon Health and Science University, Portland, Oregon

⁴Department of Biomedical Engineering, Oregon Center for Spatial Systems Biomedicine, Oregon Health and Science University, Portland, Oregon

⁵Center for Health Research, Kaiser Permanente Northwest, Portland, Oregon

Correspondence

Pepper Schedin, Department of Cell, Developmental, and Cancer Biology, Oregon Health and Science University, 2720 SW Moody Ave, Mailing Code: KR-CDCB, Portland, OR 97201.

Email: schedin@ohsu.edu

Funding information

Susan G. Komen, Grant/Award Number: PDF17480342; Oregon Clinical and Translational Research Institute; Knight Cancer Institute Pilot Grant

Abstract

A hallmark of ductal carcinoma in situ (DCIS) progression is a loss of the surrounding ductal myoepithelium. However, whether compromise in myoepithelial differentiation, rather than overt cellular loss, can be used to predict the risk of DCIS progression is unknown. Here we address this question utilizing pure and mixed DCIS cases (N = 30) as surrogates for DCIS at low and high risk for progression, respectively. We used multiplex immunohistochemical staining to evaluate the relationship between myoepithelial cell differentiation and lymphoid immune cell types associated with poor prognostic DCIS. Our results show that myoepithelial calponin-1 discriminates between pure and mixed DCIS lesions better than histological subtype, presence of necrosis, or nuclear grade. Additionally, focal loss of myoepithelial cells associated with increased PD-1+CD8+ T cells, which suggests a link between the myoepithelium and immune surveillance. To identify associations between calponin-1 expression and immune response, we performed unsupervised hierarchical clustering of myoepithelial and immune cell biomarkers on 219 DCIS lesions from 30 cases. Notably, the majority of pure (low-risk) DCIS lesions clustered in a high calponin-1, T cell low group, whereas the majority of mixed (high-risk) DCIS lesions clustered in a low calponin-1, T cell high group, specifically with CD8+ and PD-1+CD8+ T cells. However, a subset of pure DCIS lesions had a similar calponin-1 and immune signature as the majority of mixed DCIS lesions, which have low calponin-1 and T cell enrichment—raising the possibility that these pure DCIS lesions might be at a high risk for progression.

KEYWORDS

breast cancer, immune surveillance, microinvasive DCIS, myoepithelial differentiation, tumor microenvironment

Abbreviations: DCIS, ductal carcinoma in situ; FFPE, formalin-fixed, paraffin-embedded; IBC, invasive breast cancer; ER, estrogen receptor; mIHC, multiplex immunohistochemistry; SMA, α -smooth muscle actin.

This is an open access article under the terms of the Creative Commons Attribution-NonCommercial-NoDerivs License, which permits use and distribution in any medium, provided the original work is properly cited, the use is non-commercial and no modifications or adaptations are made.

© 2020 The Authors. *Molecular Carcinogenesis* published by Wiley Periodicals LLC

1 | INTRODUCTION

Ductal carcinoma in situ (DCIS) of the breast, defined by tumor cell proliferation confined to the mammary ducts, makes up approximately 20% of all breast cancers in the US.^{1,2} Current standard of care dictates that DCIS be treated the same as early-stage invasive breast cancer (IBC), even though long-term studies show that as few as approximately 30% of untreated DCIS cases progress to IBC.^{3,4} Given toxicities and co-morbidities of current treatments, which include surgery, radiotherapy, and/or endocrine therapy, there is a clinical need for biomarkers that delineate between patients at high and low risk of disease progression. Such biomarkers might reduce overtreatment in women at low risk, and identify women at high risk that are most likely to benefit from prevention strategies.⁵⁻¹⁰

To date, DCIS biomarker discovery has focused predominantly on tumor intrinsic attributes, with one study of 1492 DCIS cases identifying lesions positive for p16, COX2, and ERBB2, and negative for estrogen receptor (ER) at high risk for progression.¹¹ However, the proportion of cases with this set of characteristics was only 3%. Other studies found that somatic mutations and changes in gene expression occurred early, at the transition from normal to DCIS, and did not delineate between low- and high-risk lesions.¹²⁻¹⁹ Conversely, the tumor microenvironment of DCIS and overt IBC have significant differences in global gene expression. Consequently, research efforts to understand DCIS progression have pivoted toward the tumor microenvironment. In this paper, we investigate the possibility that the myoepithelium plays a role in the progression of DCIS by regulating the local immune response to DCIS tumor cells.

In support of a critical role for the myoepithelium in the transition of DCIS to IBC, research in murine models reveals that the myoepithelium acts as a “gatekeeper,” inhibiting tumor cell escape.^{12,20-24} Additionally, myoepithelial cells show significant gene expression changes between DCIS and IBC, including the expression of immune-modulating chemokines.^{22,25-27} Further evidence for a myoepithelial cell role in DCIS progression is the observation that myoepithelial cells show a progressive decline in differentiation markers, including p63, calponin, and α -smooth muscle actin (SMA), before actual loss of the myoepithelium.²⁸ Further, the myoepithelial protein calponin-1, a smooth muscle-associated protein, correlates with DCIS progression in murine models.²⁸ Calponin-1 is known to bind and stabilize the actin cytoskeleton in smooth muscle cells, where it contributes to force production.^{29,30} In one study, loss of expression of calponin-1 corresponded with an approximately 130-fold increased probability of adjacent tumor cells expressing a poor prognostic basal tumor cell marker.²⁸ Further, calponin-1 is included in a set of 17 genes that predicts increased risk of metastasis in breast cancer patients.^{30,31} While it is currently unknown what factors control the loss of myoepithelial cell differentiation in DCIS progression, observations showing lymphocyte infiltration concurrent with focally compromised myoepithelial cells have implicated the immune system as a possible factor.³²⁻³⁸

While numerous studies have investigated the prognostic value of immune infiltrates in IBC, how immune cells cooperate to suppress

or promote DCIS progression is an emerging field. Past studies found that specific immune cell populations associated with high-risk pathological features, such as DCIS grade, histologic subtype, and DCIS recurrence.³⁹⁻⁴⁴ However, immune markers predictive of DCIS progression and loss of myoepithelial cell integrity have not been reported. Here we investigated whether myoepithelial cell differentiation state, as defined by expression of SMA and calponin-1, associated with distinct immune milieus in DCIS. Further, we investigated whether combining biomarker data from both myoepithelial and immune cells improved the ability to delineate between DCIS populations defined as low or high risk for progression. Understanding how myoepithelial cells associate with an immune response to DCIS may help guide the application of future therapeutics for the prevention of DCIS progression, including novel approaches for immune modulation.

For the purposes of this study, we investigated microenvironmental biomarkers in cases of pure DCIS and DCIS in the background of IBC (mixed DCIS), as surrogates for low- and high-risk DCIS cohorts, respectively. The rationale for this strategy has been described by others and is based on two premises.⁴⁵⁻⁴⁷ The first premise is that pure DCIS cases are more likely to be enriched for attributes of a low-risk tumor microenvironment. The second is that DCIS cases in the background of invasive disease (mixed DCIS), but physically distant from invasive tumors, represent DCIS lesions that are more likely to progress and therefore more likely to reside in a high-risk microenvironment. To assess the myoepithelial and immune component of these respective DCIS cohorts and to determine if their tumor microenvironments are distinct, we used multiplex immunohistochemistry (mIHC). mIHC allows us to assess multiple myoepithelial differentiation markers and lymphoid immune cell populations on the same tissue section, permitting high resolution images of cell phenotype and relative spatial proximity within the context of intact tissue.

Our results suggest myoepithelial calponin-1 is a tumor-suppressive biomarker that has the ability to discriminate between low- and high-risk DCIS lesions better than histological subtype, presence of necrosis, or nuclear grade. Further, we find an association between the loss of calponin-1 expression and immune cell infiltrates consistent with an intact myoepithelium acting as a T cell barrier. Notably, the majority of pure (low-risk) DCIS lesions had high calponin-1 and an immune composition low in T cells, whereas the majority of mixed (high-risk) DCIS lesions had low calponin-1 and an enrichment for T cells, specifically CD8+ and PD-1+CD8+ T cells. However, a subset of pure DCIS lesions had a similar calponin-1 and immune signature as the majority of mixed DCIS lesions, with low calponin-1 and T cell enrichment—raising the possibility that these pure DCIS lesions might be at a high risk for progression. Cumulatively, these data show that loss of myoepithelial calponin-1 associates with an activated CD8+ T cell response and raises the possibility that myoepithelial cells mediate an immune response to DCIS. These observations support further investigation into the role of calponin-1 as a tumor-suppressive protein and mediator of the immune response, which may contribute to the development of future therapies in the prevention of DCIS progression.

2 | METHODS

2.1 | Human tissue acquisition

Formalin-fixed, paraffin-embedded (FFPE) breast tissue sections from female patients diagnosed with pure DCIS or microinvasive DCIS were obtained from the Oregon Health & Science University (OHSU) biorepository under OHSU Institutional Review Board approval. FFPE breast tissue sections from patients diagnosed with DCIS with a concurrent diagnosis of IBC (mixed DCIS) were obtained from Kaiser Permanente Northwest under a joint OHSU-Kaiser Institutional Review Board protocol. All cases were de-identified to the research team at all points.

2.2 | Multiplex immunohistochemistry

FFPE tissue sections were used for mIHC staining of a lymphoid panel, which included antibodies for both myoepithelial and lymphoid markers (Table S1). The immunohistochemistry protocol described in Tsujikawa et al was used with minor modification.⁴⁸ Before staining, antigen retrieval in Target Retrieval Solution (Dako) was performed in a pressure cooker (Pascal) at 125°C for 5 minutes. Next, slides were treated with 3% H₂O₂ in methanol for 10 minutes at room temperature to block endogenous peroxidases. For each mIHC cycle, a primary antibody was incubated at the concentration and duration shown in Table S1. Then, slides were washed in 1X Tris-buffered saline with Tween-20 buffer and incubated with pre-diluted horse-radish peroxidase (HRP)-conjugated secondary antibody (Histofine) according to manufacturer specifications. Slides were then incubated with AEC peroxidase (HRP) chromogen substrate (Vector Laboratories) per manufacturer instructions. Post-staining, slides were scanned using the Aperio Scanscope (AT2). AEC chromogen was removed with 100% ethanol. Antibody stripping was performed to remove primary-secondary antibody complexes. Antibody stripping was achieved by immersing slides in pH 6.0 citrate buffer (Biogenex) before the following microwave treatment: 90 seconds at full power to reach 100°C, then 3 minutes at 10% power, followed by 12 minutes at 20% power. A single mIHC cycle consisted of primary and secondary antibody incubation, AEC chromogen reaction, slide scanning, AEC chromogen removal, and antibody stripping. This cycle was repeated for each primary-secondary antibody combination shown in Table S1.

2.3 | Multiplex immunohistochemical image processing for pure and mixed DCIS cases

After staining, images from each cycle were analyzed using a modified image processing pipeline previously described by Tsujikawa et al.⁴⁸ Image alignment and extraction was performed using the SURF algorithm in the Computer Vision Toolbox of Matlab version R2018b (The MathWorks, Inc, Natick, MA). Single-cell segmentation

and color deconvolution was performed in FIJI,⁴⁹ and mean intensity quantification was performed in Cell Profiler version 3.5.1.^{50,51} FCS Express 6 Image Cytometry RUO (De Novo Software, Glendale, CA) was used to perform image cytometry and calculate immune cells as a percentage of total nuclei and as a percentage of CD45+ cells.

2.4 | Myoepithelial border expression

Myoepithelial expression of SMA and calponin-1 surrounding DCIS lesions were measured visually for each DCIS lesion as previously described.²⁸ Two independent researchers assessed calponin-1 expression, with a third independent assessment performed when greater than 20% discrepancy was found between researchers.

2.5 | Lesion masks and myoepithelial calponin-1 gap identification

The location of gaps in myoepithelial calponin-1 expression was visualized using previously described methods with adaptations.⁵² Two image masks were made, a myoepithelial mask using the calponin-1 mIHC image and a mask of the DCIS lesions using a combination of CK18, calponin-1, and SMA. The calponin-1 gaps were identified by creating a third mask defined as the DCIS lesion mask minus the calponin-1 mask.

2.6 | CD8 to DCIS near neighbor visualization

The grayscale mIHC images from myoepithelial and lymphoid mIHC staining of calponin, CD8, and SMA were nonlinear contrast-enhanced using the OpenCV function "cv2.morphologyEx" (<https://docs.opencv.org/>). The CellProfiler cell center coordinates from the mIHC analysis pipeline were used to draw a line from each CD8+ cell to the nearest pixel on the DCIS lesion mask.

2.7 | Histopathological evaluation

Individual DCIS-affected ducts were evaluated by pathologist S.J. for grade, necrosis, and DCIS histological and biological subtypes.

2.8 | Statistics

Statistics were performed in GraphPad Prism V8. The Mann-Whitney *U* test was used to compare calponin-1 and SMA DCIS border expression. Mixed-effects analysis with multiple comparisons was used to assess immune cell type differences between microinvasive and noninvasive stromal areas, between pure and mixed DCIS, and between DCIS lesions with low and high calponin-1 expression. χ^2 analysis was used to analyze clinical characteristics between pure

and mixed DCIS groups. The Mann-Whitney *U* test was used to analyze age differences between pure and mixed DCIS groups. R-studio was used to perform K-means clustering analysis of calponin-1 expression. The heatmap3 package was used in R-Studio to perform unsupervised hierarchical clustering.

3 | RESULTS

3.1 | Calponin-1 expression differentiates pure and mixed DCIS cases

Assessment of the clinical and pathological attributes of the pure and mixed DCIS cases analyzed in this study (Table 1) revealed no statistically significant differences between groups for patient age, grade, or histological subtype. We next determined if myoepithelial cell compromise, as defined by loss of the differentiation markers SMA or calponin-1, could distinguish between pure and mixed DCIS lesions. We analyzed 219 total lesions (~8 lesions per case) and found the myoepithelium consistently stained positive for SMA (Figure 1A, left column), as expected for a DCIS diagnosis. In contrast, myoepithelial calponin-1 expression was heterogeneous, and staining ranged from nearly complete boarder coverage

(Figure 1A, top row, right panel) to near absence (Figure 1A, bottom row, right panel). Quantitation of SMA staining confirmed expression was uniformly high, with greater than 70% positive myoepithelial border staining in all but three cases (Figure 1B). Conversely, calponin-1 expression was heterogeneous and differed between pure and mixed DCIS. Myoepithelial border calponin-1 expression was reduced in mixed DCIS cases compared with pure DCIS (Figure 1B). Loss of calponin-1 expression in the DCIS myoepithelium is a previously unreported feature of mixed DCIS and is consistent with the premise that mixed DCIS lesions reside in a higher risk tumor microenvironment.

To group DCIS lesions by calponin-1 expression, we performed a k-means cluster analysis of myoepithelial calponin-1 expression for all lesions. K-means clustering defined three levels of calponin-1 expression: low ($\leq 25\%$), medium (>25 and $\leq 65\%$), and high ($>65\%$) (Figure 1C). The low calponin-1 group was composed predominantly of mixed DCIS cases, while the high calponin-1 group was composed predominantly of pure DCIS cases (Figure 1C). We next assessed for intracase heterogeneity of calponin-1 expression. Forty percent (12/30) of all cases showed little intracase variation, with all lesions fitting predominantly within a k-means cluster (Figure 1D). Conversely, 60% (18/30) of cases showed high intracase variation, with calponin-1 expression ranging from 20% to 100%, depending on the lesion (Figure 1D). Altogether, these data show that while calponin-1 expression differs between pure and mixed DCIS cases, calponin-1 loss is common, suggesting that calponin-1 expression is not sufficient to delineate between lesions at low and high risk of progression.

TABLE 1 DCIS clinical characteristics

# Of cases	Group		P value
	Pure DCIS 19	Mixed DCIS/IBC 11	
Average age	57.2	47.4	.1053
Age range (max/min)	(83/31)	(68/33)	
Biological subtype			.1768
Luminal A	12 (63.1%)	6 (54.5%)	
Luminal B	6 (31.6%)	2 (18.2%)	
Her2+	1 (5.3%)	0	
TNBC	0	1 (9.1%)	
Missing	0	2 (18.2%)	
Presence of necrosis	11 (57.8%)	5 (45.5%)	.5104
Nuclear grade			.8615
Grade 1	6 (31.5%)	3 (27.2%)	
Grade 2	6 (31.5%)	5 (45.5%)	
Grade 3	7 (36.8%)	3 (27.2%)	
Histological type			.9212
Papillary	2 (10.5%)	0	
Micropapillary	3 (15.8%)	2 (18.2%)	
Apocrine	1 (5.3%)	1 (9.1%)	
Comedo	5 (26.3%)	3 (27.3%)	
Solid	5 (26.3%)	4 (36.3%)	
Cribiform	3 (15.8%)	1 (9.1%)	

Note: χ^2 analysis was used for biological subtype, necrosis, grade, and architectural type. The Mann-Whitney *U* test used for age range analysis. Abbreviations: DCIS, ductal carcinoma in situ; Her2, human epidermal growth factor receptor 2; IBC, invasive breast cancer; TNBC, triple-negative breast cancer.

3.2 | PD-1 activated CD8+ T cells associate with microinvasive DCIS foci

We next assessed for an association between myoepithelial cell differentiation state and the local immune composition, which might implicate a functional link between these distinct compartments of the microenvironment. We first investigated this relationship in DCIS cases with focal loss of the myoepithelium and microinvasion, as these cases have a twofold increased risk of progression to IBC compared to DCIS without microinvasion.⁵³ Further, immune cell infiltrates have been described with microinvasion, suggesting immune cells could be biomarkers of DCIS progression.^{35–38,54} We focused our analysis on the lymphoid immune populations, as past studies have associated increased numbers of T and B cells with high-grade DCIS lesions and recurrence.^{41,55,56} We employed mIHC to analyze 10 lymphoid cell markers, two myoepithelial cell markers (SMA and calponin), and one tumor cell marker (CK18) within the same tissue section. A representative single IHC image for each biomarker is shown in Figure S1. We compared regions of focal microinvasion (Figure 2A, blue-outlined area) to noninvasive stromal border regions within the same DCIS lesion (Figure 2A, pink-outlined area minus blue-outlined area) and used image cytometry to capture the immune cell populations (Figure 2B). Figure 2C shows a representative pseudocolored mIHC image of a DCIS lesion with a microinvasive foci, as evidenced by a loss of the myoepithelial cell

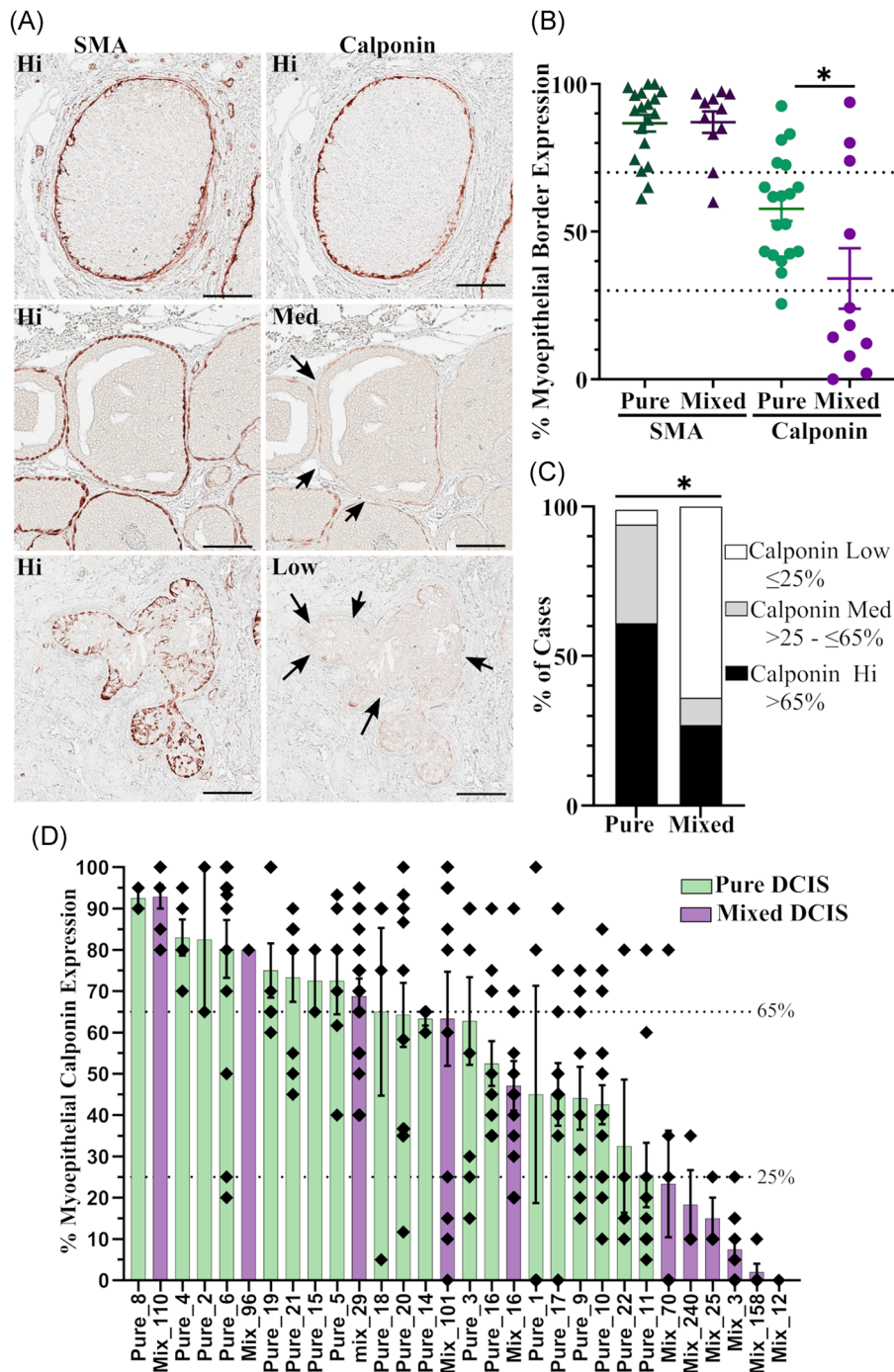


FIGURE 1 Mixed DCIS lesions show loss of myoepithelial calponin-1 expression compared with pure DCIS. Thirty DCIS cases were stained using multiplex IHC for myoepithelial markers calponin-1 and SMA. A, Representative single-channel IHC images of DCIS lesions show high SMA DCIS myoepithelial border expression in most lesions; calponin-1 expression (right panel) was heterogeneous with high (top) medium (middle) and low (bottom) expression shown. Arrows point to gaps in calponin-1 staining. B, The percentage of DCIS myoepithelial border expression was determined for each DCIS lesion (~8 lesions/case, $n = 219$ lesions total) for both SMA and calponin-1. Mixed DCIS had significantly reduced calponin-1 expression compared with pure DCIS, while SMA expression was similar in both (the Mann-Whitney U test, $P < .05$). C, K-means clustering was used to group calponin-1 expression into three clusters (high, medium, and low). Pure DCIS cases were found predominantly in the high calponin-1 group while mixed DCIS cases were found mostly in the calponin-1 low group (K-means clustering in R-studio). The Mann-Whitney U test, $P < .05$. D, DCIS lesions within each case displayed heterogeneous calponin-1 expression with 60% (18/30) of cases showing high intracase variation. Dotted lines show k-means cutoff values for calponin-1 expression. Scale bars are 100 μm . DCIS, ductal carcinoma in situ; IHC, immunohistochemistry; SMA, α -smooth muscle actin

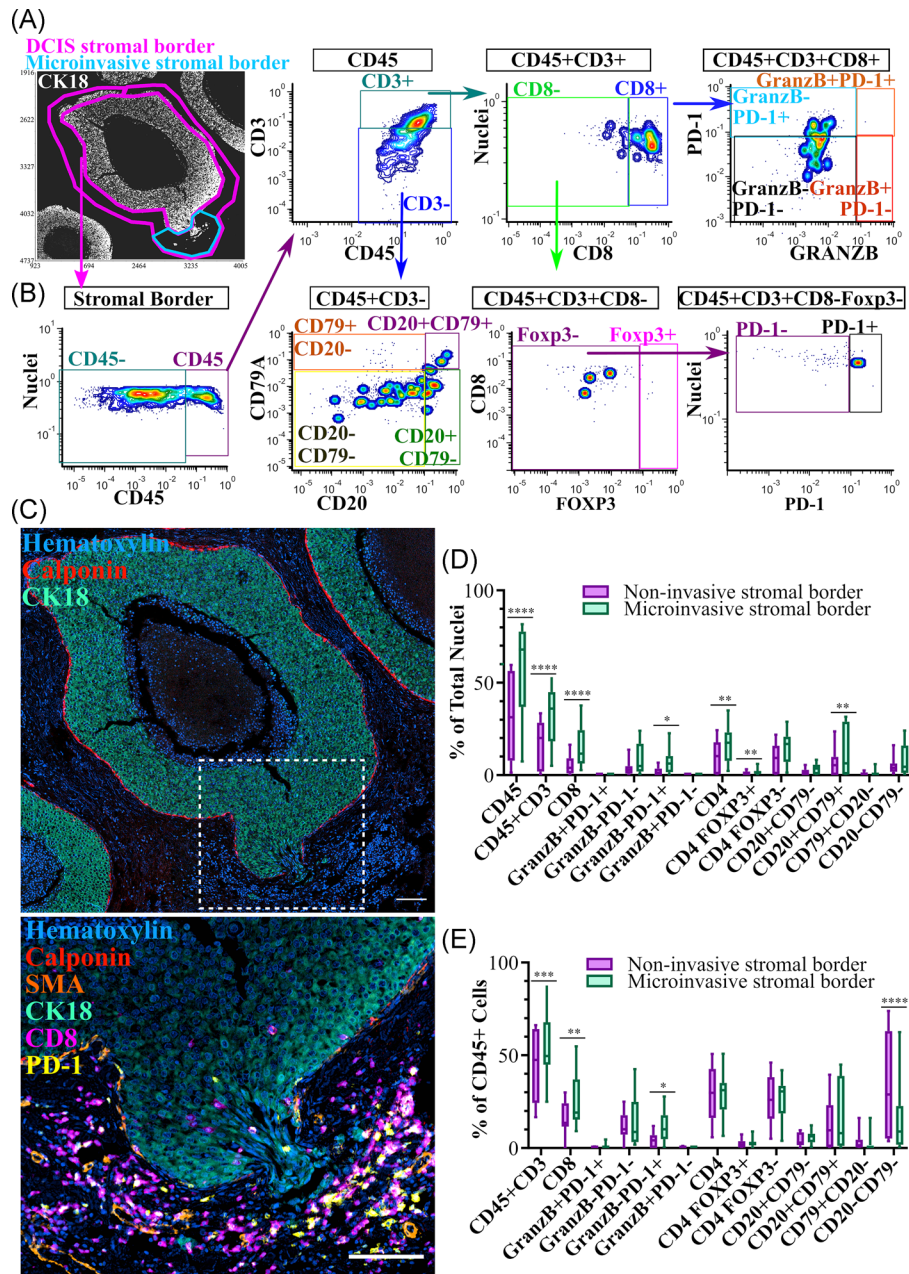


FIGURE 2 Microinvasive DCIS foci show increased immune infiltrates with enrichment for T cells and an increased frequency of PD-1+CD8+ T cells. The immune composition was assessed in DCIS areas with microinvasion compared with noninvasive areas of the same lesion ($n = 10$ cases of DCIS, $n = 32$ microinvasive areas). A, ROI selected for both the microinvasive area (blue outline) and the noninvasive area of the same lesion (pink outline) shown against CK18 stain. B, FCS Image Cytometry gating scheme. CD45+ immune cells were captured within the DCIS stromal border region. The CD45+CD3- gate was used to capture all non-T cells, which were characterized for the B cell markers CD20 and CD79a. A CD45+CD3+ gate was used to capture T cells; we next assessed for CD8 positivity and then characterized this population for expression of the activation markers granzyme B and PD-1. CD4+ T cells were defined by the CD45+CD3+CD8- gate, which were further characterized for FOXP3 positivity to identify CD4+ T regulatory cells and for PD-1 positivity to assess activation state. C, Multiplex IHC images of a microinvasive area stained for myoepithelial and lymphoid markers. Top image shows hematoxylin (blue), calponin-1 (red), and CK18 (teal). The bottom image shows an enlarged area of the white boxed region with hematoxylin (blue), calponin-1 (red), SMA (orange), CK18 (teal), CD8 (pink), and PD-1 (yellow). D, Microinvasive regions showed an increased number of CD45+ cells, T cells, CD8+ T cells, CD4+ T cells, PD-1+CD8+ T cells, and an increased number of CD20+CD79+ B cells. E, PD-1+CD8+ T cells were significantly increased as a percentage of total immune infiltrate. GraphPad Prism 8 was used to calculate mixed-effects analysis with multiple comparisons. * $P < .05$, ** $P < .01$, *** $P < .001$, and **** $P < .0001$. Scale bars are 100 μm . DCIS, ductal carcinoma in situ; FCS, flow cytometry standard; IHC, immunohistochemistry; ROI, region of interest; SMA, α -smooth muscle actin

layer and invasion of CK18+ tumor cells (albeit with reduced staining compared with the noninvasive tumor cells) into the adjacent stroma (Figure 2C, top panel). An enlarged image of the microinvasive area stained for CD45+ immune cells and PD-1+CD8+ T cells is shown (Figure 2C, bottom panel). Quantitative analysis of 10 microinvasive cases revealed increased CD45+ immune infiltration, as well as an increase in CD3+ T cells, specifically CD8+ T cells and PD-1+CD8+ T cells, compared with noninvasive regions of the same lesion (Figure 2D). An influx of CD20+CD79a+ B cells is also observed. To determine whether immune cell phenotypes differ between microinvasive and noninvasive regions, we next assessed immune cell populations as a percentage of CD45+ cells. We find that CD8+ and PD-1+CD8+ T cells are significantly increased in microinvasive regions compared with noninvasive regions (Figure 2E). Altogether, these results show that focal loss of the myoepithelial cell layer is associated with a lymphoid signature that is indicative of both inflammation (increased CD45+ cells as a percent of total nuclei) and enrichment for PD-1 activated CD8+ T cells (as a percent of CD45+ cells).

3.3 | Mixed DCIS have reduced immune cell numbers compared with pure DCIS

Having found an influx of immune cells in areas of focal loss of the myoepithelium, we next determined if the immune milieu of the stromal microenvironment differed between mixed and pure DCIS lesions. We focused our analysis on lymphoid cell populations within DCIS lesions and in the nearby stromal border (~50-80 μ m); our image cytometry approach for this analysis is shown in Figure S2. We found that mixed and pure DCIS were differentiated by the total number of CD45+ immune cells, but contrary to our initial expectations, mixed DCIS lesions had significantly fewer immune cells compared with pure DCIS lesions (Figure 3A). Overall, mixed DCIS

lesions had reduced CD45+CD3+ T cells and FOXP3+CD8- T regulatory T cells (Figure 3A).

3.4 | Majority of CD8+ T cells in mixed DCIS have PD-1 activation

We next assessed for specific immune populations based on the percentage of CD45+ cells rather than total nuclei. We found an enrichment of CD3+ T cells, CD4+ T cells, and CD8+ T cells in mixed DCIS lesions compared with pure DCIS lesions (Figure 3B). Further mixed DCIS lesions had increases in PD-1+CD8+ T cells as a percentage of CD45+ immune cells. Further, regulatory T cells were low in mixed DCIS lesions compared with pure, both as a percent of total nuclei and as a percent of CD45+ immune cells. Together these data suggest that the abundance of immune cells in mixed DCIS is reduced compared with pure DCIS lesions; however, the composition of the lymphoid immune milieu in mixed DCIS lesions is similar to microinvasive DCIS, with enrichment for activated PD-1+CD8+ T cells.

3.5 | DCIS lesions with low calponin-1 have an immune composition enriched for PD-1+CD8+ T cells

To assess if the loss of myoepithelial calponin-1 expression associates with a specific immune profile, we grouped pure and mixed DCIS lesions together and compared DCIS lesions in the K-means high calponin-1 group (>65% calponin-1 expression) to those in the K-means low calponin-1 group (\leq 25% calponin-1 expression) (Figure 1C). We focused on the low and high calponin-1 groups as a proof-of-principal study, as we predict near-complete loss of calponin-1 in the myoepithelium to associate with an immune response distinct from that observed in DCIS lesions with full calponin-1 expression. As a percent of total nuclei, there

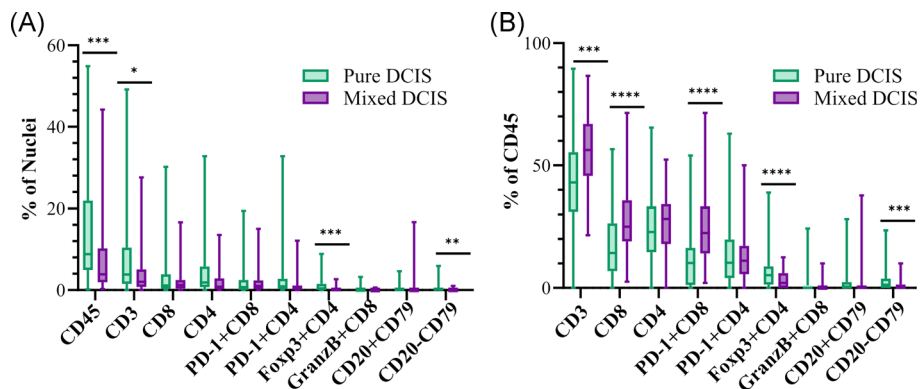


FIGURE 3 Mixed DCIS has a reduced lymphoid infiltrate with an immune composition enriched for PD-1+CD8+ T cells compared with pure DCIS. A, Lymphoid immune cell populations within DCIS lesions from both mixed and pure DCIS were quantified using image cytometry. CD45, CD3, CD8, and CD4 populations were measured as a percentage of total nuclei. B, Immune composition is shown as a percentage of CD45+ cells. Leukocyte infiltration in mixed DCIS was significantly less than pure DCIS, with a lower number of T cells and CD8+ T cells but with fewer FOXP3+ cells. Immune composition of mixed DCIS was enriched for T cells and CD8+ T cells, PD-1+CD8+ T cells yet a decreased composition of FOXP3+ cells. GraphPad Prism 8 was used to calculate mixed-effects analysis with multiple comparisons. DCIS, ductal carcinoma in situ.

* $P < .05$, ** $P < .01$, *** $P < .001$, and **** $P < .0001$

was no significant difference in CD45+ immune cells or in CD45+CD3+ T cells between the high and low calponin-1 groups (Figure 4A). However, when we assessed the immune cell populations as a percentage of total CD45+ cells, we found significant enrichment of CD3+ T cells, CD8+ T cells, and activated PD-1+CD8+ T cells in the calponin-1 low group compared with the calponin-1 high group (Figure 4B). Together, these data indicate that low calponin-1 is associated with an enrichment for activated PD-1+CD8+ T cells, which are associated with an active immune response. Further evidence that calponin-1 expressing myoepithelial cells may serve as a barrier between DCIS tumor cells and cytotoxic T cells is suggested by nearest neighbor visualization, which

showed that CD8+ T cells were adjacent to calponin-1 positive myoepithelium, but absent within the tumor mass (Figure 4C, top right and 4D). In contrast, lesions with low calponin-1 showed increased CD8+ T cell infiltration into the DCIS tumor mass (Figure 4C, bottom right).

3.6 | Hierarchical clustering identifies four DCIS clusters

We next assessed the impact of combining the myoepithelial and lymphoid immune biomarker data on DCIS sub-grouping. We

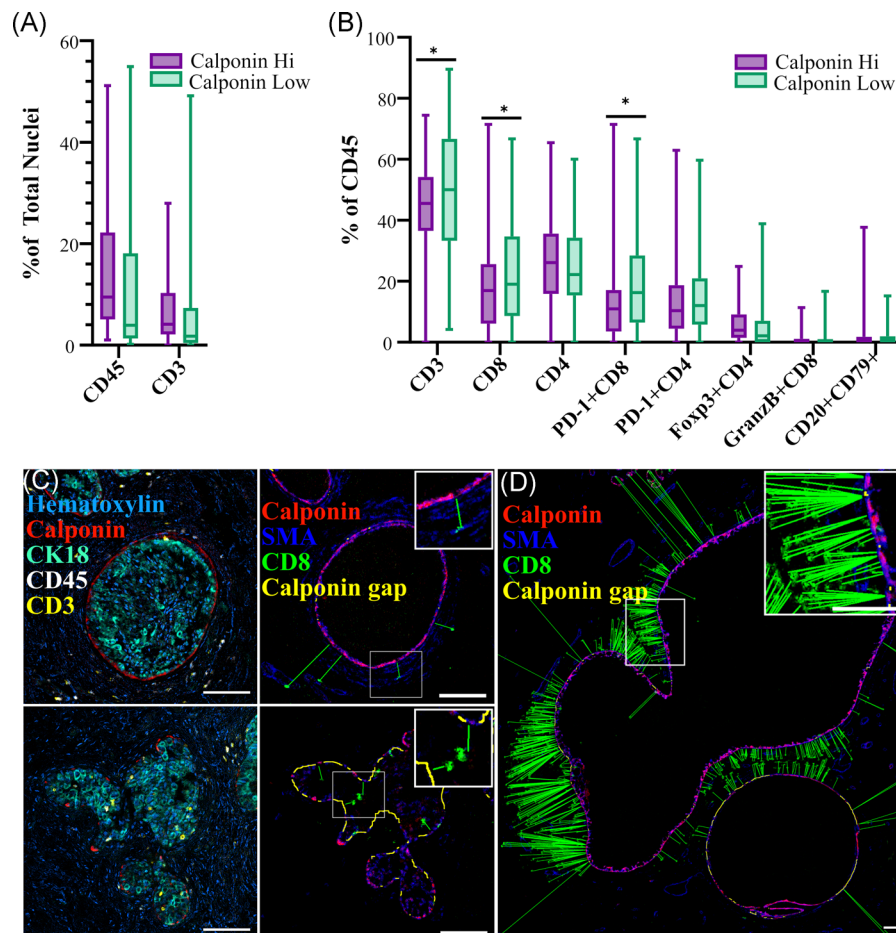


FIGURE 4 PD-1+CD8+ T cells associated with loss of myoepithelial calponin-1 expression in DCIS. DCIS lesions with the highest calponin-1 expression by k-means (>65%) were compared with lesions in the lowest k-means cluster of calponin-1 expression ($\leq 25\%$). A, DCIS lesions that have low myoepithelial calponin-1 are not significantly different from those with high calponin-1 in terms of total immune or T cell infiltrate as a percent of total nuclei. B, DCIS lesions that have low myoepithelial calponin-1 expression show an immune composition enriched for T cells, CD8+ T cells, and PD-1+CD8+ T cells. C, Left column shows representative DCIS lesions from calponin-1 high group (top panel) and calponin-1 low group (bottom panel) with hematoxylin (blue), calponin-1 (red), CK18 (teal), CD45 (white), and CD3 (yellow). The right column shows the same lesion as left column. Images show myoepithelial differentiation markers calponin-1 (red) and SMA (blue), CD8+ cells (green), and CD8+ nearest neighbor visualization, shown with green lines drawn from CD8+ cells to the nearest myoepithelial neighbor and yellow lines indicating DCIS myoepithelium with gaps in calponin-1 expression. Top and bottom rows show the same tissue section. Insets show enlarged areas of white boxed regions. D, Additional DCIS lesion with calponin-1 (red), SMA (blue), CD8 (green), and CD8+ cell nearest neighbor analysis with green lines drawn to nearest myoepithelial border pixel neighbor. CD8+ T cells are found almost exclusively outside this DCIS lesion with high calponin-1 expression. Insets show enlarged areas of white boxed regions. GraphPad Prism 8 was used to perform mixed-effects analysis with multiple comparisons. * $P < .05$, ** $P < .01$, *** $P < .001$, and **** $P < .0001$. Scale bars are 100 μm . DCIS, ductal carcinoma in situ; SMA, α -smooth muscle actin

performed an unsupervised hierarchical clustering analysis of pure and mixed DCIS lesions using SMA, calponin-1, and lymphoid immune cell populations as a percentage of CD45+ immune cells (Figure 5). This analysis sub-grouped DCIS lesions into four major clusters, with myoepithelial calponin-1 and SMA expression as primary discriminators and immune cell populations as secondary discriminators. Cluster 1 is characterized by low calponin-1 and SMA expression and enrichment for CD3+, CD8+, and PD-1+CD8+ T cells, consistent with a myoepithelial immune barrier function. Notably, cluster 1 predominantly contained mixed DCIS lesions. In cluster 2, we found DCIS lesions with low calponin-1 expression and concurrent enrichment in CD4+ T cells and PD-1+CD4+ T cells, suggestive of activated T helper cells.⁵⁷ Cluster 3 had low calponin-1 expression with enrichment for non-T cells (CD45+CD3- cells). Notably, this CD45+CD3- rich cluster is also not enriched for B cell markers (CD20 or CD79), suggesting a myeloid population. Thus, distinct immune milieus with infiltrates enriched for either CD8+, CD4+, or a CD3- immune cells were found in the three clusters with compromised myoepithelium, as defined by low calponin-1 expression.

Cluster 4 was largely defined by high calponin-1 expression and comprised mostly pure DCIS lesions. Further, these lesions were not strongly enriched for CD3+ T cells, B cells, or putative myeloid (CD45+CD3-) cells. However, the CD3+ T cells that were present consisted mostly of CD4+ T cells and FOXP3+CD4+ regulatory

T cells. These immune profiles are consistent with a noninflammatory state. In sum, this analysis showed that mixed DCIS lesions associated with a unique signature of low myoepithelial calponin-1 expression, inflammation, and immune activation while pure DCIS lesions associated with high myoepithelial calponin-1 expression, low immune cell infiltrates, and the presence of regulatory CD4+ T cells.

4 | DISCUSSION/CONCLUSION

Here we asked whether compromise in the myoepithelial cell layer, combined with specific lymphoid populations, could delineate the risk of progression in DCIS lesions. For this study, we utilized pure and mixed DCIS as surrogates for DCIS lesions at low and high risk for progression, respectively.⁴⁵⁻⁴⁷ This approach is common given the lack of large retrospective or prospective DCIS studies with long-term follow-up. Our work identifies that the myoepithelial protein calponin-1 can discriminate between pure and mixed DCIS with significantly greater resolution than tumor grade, necrosis, or histological subtype (Table 1; Figure 1). Additionally, we find that calponin-1 loss associates with an immune composition enriched for PD-1+CD8+ T cells, which suggests immune cell activation and possible exhaustion. Further, we found this association regularly in the high-risk microenvironment of mixed DCIS and within a subset of pure DCIS. These data suggest the possibility that the combination of loss of myoepithelial calponin-1 and enrichment for PD-1+CD8+ T cells may identify pure DCIS at high risk for progression. In sum, these studies support a new barrier function for the myoepithelium, with calponin-1 potentially acting as a mediator of immune infiltration.

This study combines two previously isolated microenvironmental factors in DCIS progression: myoepithelial differentiation and immune cell infiltration. Our finding that mixed DCIS has significantly reduced myoepithelial calponin-1 compared with pure DCIS agrees with the literature describing the loss of other myoepithelial differentiation markers, such as CD10, P-cadherin, and SMA, as a feature of high-risk DCIS.^{58,59} However, how calponin-1 is regulated in the mammary gland remains an open question. More is known about calponin-1's function in smooth muscle cells, where it plays a role in the stabilization of the actin cytoskeleton and the regulation of smooth muscle contractility. In smooth muscle cells, calponin-1 expression is regulated by changes in extracellular matrix tension through the transforming growth factor β (TGF- β) signaling pathway.⁶⁰ In DCIS lesions, tumor cells may exert increased force on myoepithelial cells, increasing extracellular matrix tension and triggering changes in calponin-1 expression through TGF- β signaling. Over time, this may result in reduced stability of the actin cytoskeleton of the myoepithelium, which could negatively impact myoepithelial barrier function and increase myoepithelial cell layer permeability. These changes in calponin-1 expression may impact immune surveillance of the DCIS tumor cells, either through immune cells permeating the myoepithelial layer or increased cross-talk across the myoepithelial layer. Consistent with potential cross-talk,

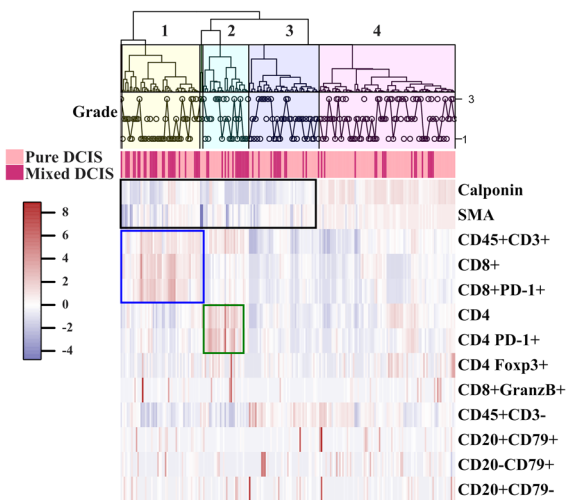


FIGURE 5 Hierarchical clustering reveals unique myoepithelial profiles in pure and mixed DCIS lesions which further correlate with distinct lymphoid populations. DCIS lesion immune cell data were input into R for hierarchical clustering as a percent of CD45. The unsupervised hierarchical analysis shows SMA and calponin-1 were the strongest discriminators between pure and mixed DCIS lesions (black box). Further, pure DCIS lesions grouped with mixed DCIS lesions (yellow and blue clusters on left) have reduced calponin-1 and SMA and higher levels of CD3+, CD8+, and PD-1+CD8+ T cells (blue box) compared with other clusters. These lesions also had higher CD4+ and PD-1+CD4+ T cells (green box). Two-hundred and nineteen lesions were analyzed from 30 DCIS cases (~8 lesions/case). DCIS, ductal carcinoma in situ; SMA, α -smooth muscle actin

myoepithelial cells associated with DCIS are known to express immune-regulating chemokines and proinflammatory factors and are enriched for immune-related signaling pathways.^{26,61,62}

In support of a potential role for the myoepithelium in regulating the immune response to DCIS lesions, we found that low calponin-1 expression was associated with a similar immune composition in pure DCIS, mixed DCIS, and microinvasive foci. Specifically, we found that microinvasive regions with focal loss of the myoepithelial layer had an increase in total immune infiltration with a lymphoid signature similar to mixed DCIS, including enrichment for CD8+ T cells and PD-1+CD8+ T cells (Figures 2 and 3). These observations are consistent with previous reports of microinvasive areas showing an influx of immune cells at sites of focal invasion.^{33–37,63} Further, one study demonstrated that microinvasive DCIS had increased infiltration of CD8+ T cells and a concomitant increase in PD-L1 expression and PD-1+CD8+ T cells compared with DCIS without microinvasion, which is consistent with our findings.⁴³ They concluded that during invasive progression, cytotoxic T cells interact with the tumor tissue, which may result in upregulation of immunosuppressive checkpoint proteins.⁴³

Supporting that CD8+ T cell infiltrate is a marker of a high-risk microenvironment in DCIS lesions, high numbers of CD8+ T cells have been reported in Her2+ and triple-negative breast DCIS, two poor prognostic subtypes.⁴⁰ Interestingly, this study also associated high numbers of immune infiltrates and CD8+ T cells with spontaneous but incomplete tumor regression, supportive of an immune response that has become exhausted.⁴⁰ Of potential relevance, others have reported a low number of CD8+HLADR+ cells associated with a high risk of ipsilateral recurrence, suggesting that T cell activation is protective.⁵⁶ Cumulatively, these and other studies highlight the potential heterogeneity of the immune response to DCIS lesions.^{44,56,64} Of note, how the immune response to DCIS is regulated remains under investigation, and these studies have not included an assessment of the myoepithelium in modulating this biology.

Our hierarchical clustering analysis identified a cluster of pure and mixed DCIS lesions characterized by shared immune and myoepithelial signatures. Specifically, this cluster of lesions expressed low calponin-1 and was enriched for PD-1+CD8+ T cells. Even though a PD-1+CD8+ T cell population usually indicates clonal expansion and activation, the presence of this population in DCIS with low calponin-1 is consistent with studies that show a dysfunctional CD8+ T cell response caused by the persistence of tumor antigens.⁶⁵ Further T cell phenotyping would be necessary to confirm exhaustion.

In support of immune cell exhaustion in high-risk DCIS lesions, a recent model of immune avoidance in DCIS progression proposes that few tumor cells interact with immune cells due to physical separation by the myoepithelial layer and basement membrane.³⁷ One prediction based on this model is that increased immune cell infiltrate would be observed in IBC compared with DCIS. However, compared with IBC, DCIS cases have increased CD8+ T cells, increased TIGIT-expressing CD8+ T cells, and a high diversity of TCR clonotypes, hallmarks of immune activation.³⁷ One possibility is that initial tumor cell breach of the myoepithelial layer triggers an

immune response that becomes exhausted by the IBC stage. Our data showing increased PD-1+CD8+ T cell activation in low calponin-1 DCIS lesions expand this model by suggesting that reduced myoepithelial barrier function, rather than a physical breach, may be sufficient to expose tumor cells to immune surveillance and lead to eventual immune cell exhaustion.

Although our cohort was selected to help us distinguish between low- and high-risk DCIS lesions, our pure DCIS cases lack long-term outcomes and our mixed DCIS cases are in the background of IBC, which may impact results. Additionally, the majority of our DCIS cases are ER+, which limits our ability to predict if this unique association between the myoepithelium and immune cells is applicable to ER- or Her2+ subtypes. Further, our data indicate a relationship between myoepithelial calponin-1 and immune cell activation, but the directionality of this relationship remains an open question. We hypothesize that DCIS tumor cells may exert increased force on the myoepithelial cell layer, impacting calponin-1 expression. However, it is also possible that immune cell response to the tumor may compromise myoepithelial cell calponin-1 expression. In support of immune cell signaling affecting myoepithelial differentiation, studies show that T and B cells can secrete interferon- γ , a cytokine that has been shown to repress calponin-1 expression in vascular smooth muscle cells.^{66,67} Animal models of mammary myoepithelial cell calponin-1 knock out and assessment of PD-1+CD8+ T cells and myoepithelial calponin-1 expression in a large cohort of retrospective DCIS tissue with outcomes data would shed light on the role of myoepithelial calponin-1 in DCIS progression and immune response. Additionally, unlike previous studies evaluating immune cell populations in DCIS, we did not find any correlation between immune populations and DCIS subtype or grade. However, this analysis was limited by our sample size.

In this study, we find that calponin-1 expression alone is a better discriminator of pure and mixed DCIS than tumor biologic subtype or grade, supporting the perspective that calponin-1 may be a biomarker of DCIS progression. Further, we find a link between myoepithelial cell differentiation and immune activation state, which raises the formal possibility that modulation of myoepithelial calponin-1 expression leads to changes in immune activation. This concept that myoepithelial cells may regulate the immune milieu in the mammary gland, while novel, would be consistent with the role of immune modulation by other mammary cell types including normal fibroblasts.⁶⁸ Further research into myoepithelial barrier function and its relationship with the immune response to DCIS is warranted. Understanding the biology behind myoepithelial cell differentiation may help guide the application of future therapeutics, including novel approaches to immune modulation for the prevention of DCIS progression.

ACKNOWLEDGMENTS

The authors wish to acknowledge the contributions of Weston Anderson for the excellent support in drafting, review, and editing of the manuscript; Nathan Pennock for critical review of data; and Drs. Lisa Coussens and Takahiro Tsujikawa for training and consultation for multiplex immunohistochemistry.

CONFLICT OF INTERESTS

The authors declare that there are no conflict of interests.

DATA AVAILABILITY STATEMENT

The data that support the findings of this study are available from the corresponding author upon reasonable request.

ORCID

Pepper Schedin  <http://orcid.org/0000-0003-4244-987X>

REFERENCES

- American Cancer Society. *Breast Cancer Facts & Figures 2017-2018*. Atlanta: American Cancer Society, Inc. 2017.
- Ward EM, DeSantis CE, Lin CC, et al. Cancer statistics: breast cancer in situ. *CA Cancer J Clin*. 2015;65(6):481-495.
- Sanders ME, Schuyler PA, Simpson JF, Page DL, Dupont WD. Continued observation of the natural history of low-grade ductal carcinoma in situ reaffirms proclivity for local recurrence even after more than 30 years of follow-up. *Mod Pathol*. 2014;28(5):662-669.
- Page DL, Dupont WD, Rogers LW, Jensen RA, Schuyler PA. Continued local recurrence of carcinoma 15-25 years after a diagnosis of low grade ductal carcinoma in situ of the breast treated only by biopsy. *Cancer*. 1995;76(7):1197-1200.
- Whelan TJ, Pignol JP, Levine MN, et al. Long-term results of hypofractionated radiation therapy for breast cancer. *N Engl J Med*. 2010;362(6):513-520.
- Newman LA, Bensenhaver JM. History of ductal carcinoma in situ management based upon data from prospective, randomized clinical trials. In: Newman LA, Bensenhaver JM, eds. *Ductal Carcinoma In Situ and Microinvasive/Borderline Breast Cancer*. New York, NY: Springer New York; 2015:57-65.
- Shah C, Wobb J, Manyam B, et al. Management of ductal carcinoma in situ of the breast: a review. *JAMA Oncol*. 2016;2(8):1083-1088.
- Narod SA, Iqbal J, Giannakeas V, Sopik V, Sun P. Breast cancer mortality after a diagnosis of ductal carcinoma in situ. *JAMA oncology*. 2015;1(7):888-896.
- John MSB, Sharon N-M, Eileen R. Ductal carcinoma in situ of the breast: can biomarkers improve current management? *Clin Chem*. 2013;60(1):60-67.
- Laura LR, Parijatham SS, Dawn H, et al. Breast cancer chemoprevention among high-risk women and those with ductal carcinoma in situ. *Breast J*. 2015;21(4):377-386.
- Annette MM, Jennette DS, Britt-Marie L, Thea DT, Karla K. Risk prediction for local versus regional/metastatic tumors after initial ductal carcinoma in situ diagnosis treated by lumpectomy. *Breast Cancer Res Treat*. 2016;157(2):351-361.
- Hu M, Peluffo G, Chen H, Gelman R, Schnitt S, Polyak K. Role of COX-2 in epithelial-stromal cell interactions and progression of ductal carcinoma in situ of the breast. *Proc Natl Acad Sci USA*. 2009;106(9):3372-3377.
- Schnitt SJ. The transition from ductal carcinoma in situ to invasive breast cancer: the other side of the coin. *Breast Cancer Res*. 2009;11(1):101.
- Johnson CE, Gorringer KL, Thompson ER, et al. Identification of copy number alterations associated with the progression of DCIS to invasive ductal carcinoma. *Breast Cancer Res Treat*. 2012;133(3):889-898.
- Bombonati A, Sgroi DC. The molecular pathology of breast cancer progression. *J Pathol*. 2011;223(2):307-317.
- Abba MC, Gong T, Lu Y, et al. A molecular portrait of high-grade ductal carcinoma in situ. *Cancer Res*. 2015;75(18):3980-3990.
- Castro NP, Osório CA, Torres C, et al. Evidence that molecular changes in cells occur before morphological alterations during the progression of breast ductal carcinoma. *Breast Cancer Res*. 2008;10(5):R87.
- Casasent AK, Schalck A, Gao R, et al. Multiclonal invasion in breast tumors identified by topographic single cell sequencing. *Cell*. 2018;172(1-2):205-217. e212.
- Pang JM, Dobrovic A, Fox SB. DNA methylation in ductal carcinoma in situ of the breast. *Breast Cancer Res*. 2013;15(3):206.
- Jones JL, Shaw JA, Pringle JH, Walker RA. Primary breast myoepithelial cells exert an invasion-suppressor effect on breast cancer cells via paracrine down-regulation of MMP expression in fibroblasts and tumour cells. *J Pathol*. 2003;201(4):562-572.
- Bodicoat DH, Schoemaker MJ, Jones ME, et al. Loss of MMP-8 in ductal carcinoma in situ (DCIS)-associated myoepithelial cells contributes to tumour promotion through altered adhesive and proteolytic function. *Breast Cancer Res*. 2017;19(1):19.
- Hu M, Yao J, Carroll DK, et al. Regulation of in situ to invasive breast carcinoma transition. *Cancer Cell*. 2008;13(5):394-406.
- Duivenvoorden HM, Rautela J, Edgington-Mitchell LE, et al. Myoepithelial cell-specific expression of stefin A as a suppressor of early breast cancer invasion. *J Pathol*. 2017;243:496-509.
- Adriance MC, Inman JL, Petersen OW, Bissell MJ. Myoepithelial cells: good fences make good neighbors. *Breast Cancer Res*. 2005;7(5):1-8.
- Barsky SH. Myoepithelial mRNA expression profiling reveals a common tumor-suppressor phenotype. *Exp Mol Pathol*. 2003;74(2):113-122.
- Allinen M, Beroukhim R, Cai L, et al. Molecular characterization of the tumor microenvironment in breast cancer. *Cancer Cell*. 2004;6(1):17-32.
- Ma XJ, Salunga R, Tuggle JT, et al. Gene expression profiles of human breast cancer progression. *Proc Natl Acad Sci USA*. 2003;100(10):5974-5979.
- Russell TD, Jindal S, Agunbiade S, et al. Myoepithelial cell differentiation markers in ductal carcinoma in situ progression. *Am J Pathol*. 2015;185:3076-3089.
- Winder SJ, Walsh MP. Smooth muscle calponin. Inhibition of actomyosin MgATPase and regulation by phosphorylation. *J Biol Chem*. 1990;265(17):10148-10155.
- Taniguchi Si. Suppression of cancer phenotypes through a multi-functional actin-binding protein, calponin, that attacks cancer cells and simultaneously protects the host from invasion. *Cancer Sci*. 2005;96(11):738-746-746.
- Ramaswamy S, Ross KN, Lander ES, Golub TR. A molecular signature of metastasis in primary solid tumors. *Nat Genet*. 2003;33(1):49-54.
- Man Y-g, Sang Q-XA. The significance of focal myoepithelial cell layer disruptions in human breast tumor invasion: a paradigm shift from the "protease-centered" hypothesis. *Exp Cell Res*. 2004;301(2):103-118.
- Man Y, Zhang Y, Shen T, et al. cDNA expression profiling reveals elevated gene expression in cell clusters overlying focally disrupted myoepithelial cell layers: implications for breast tumor invasion. *Breast Cancer Res Treat*. 2005;89(2):199-208.
- Man YG, Shen T, Weisz J, et al. A subset of in situ breast tumor cell clusters lacks expression of proliferation and progression related markers but shows signs of stromal and vascular invasion. *Cancer Detect Prev*. 2005;29(4):323-331.
- Man Y-g. Focal degeneration of aged or injured myoepithelial cells and the resultant auto-immunoreactions are trigger factors for breast tumor invasion. *Med Hypotheses*. 2007;69(6):1340-1357.
- Song G, Hsiao H, Wang JL, et al. Differential impact of tumor-infiltrating immune cells on basal and luminal cells: implications for tumor invasion and metastasis. *Anticancer Res*. 2014;34(11):6363-6380.
- Del Alcazar CRG, Huh SJ, Ekram MB, et al. Immune escape in breast cancer during in situ to invasive carcinoma transition. *Cancer Discov*. 2017;7(10):1098-1115.

38. Kim A, Heo SH, Kim YA, Gong G, Jin Lee H. An examination of the local cellular immune response to examples of both ductal carcinoma in situ (DCIS) of the breast and dcis with microinvasion, with emphasis on tertiary lymphoid structures and tumor infiltrating lymphocytes. *Am J Clin Pathol*. 2016;146(1):137-144.
39. Campbell MJ, Baehner F, O'Meara T, et al. Characterizing the immune microenvironment in high-risk ductal carcinoma in situ of the breast. *Breast Cancer Res Treat*. 2017;161(1):17-28.
40. Morita M, Yamaguchi R, Tanaka M, et al. CD8(+) tumor-infiltrating lymphocytes contribute to spontaneous "healing" in HER2-positive ductal carcinoma in situ. *Cancer Med*. 2016;5(7):1607-1618.
41. Miligy I, Mohan P, Gaber A, et al. Prognostic significance of tumour infiltrating B lymphocytes in breast ductal carcinoma in situ. *Histopathology*. 2017;71(2):258-268.
42. Thompson E, Taube JM, Elwood H, et al. The immune microenvironment of breast ductal carcinoma in situ. *Mod Pathol*. 2016;29(3):249-258.
43. Lv S, Wang S, Qiao G, et al. Functional CD3+ CD8+ PD-1- T cells accumulation and PD-L1 expression increases during tumor invasion in DCIS of the breast. *Clin Breast Cancer*. 2019;19:e617-e623.
44. Tower H, Ruppert M, Britt K. The immune microenvironment of breast cancer progression. *Cancers*. 2019;11(9):1375.
45. Buckley N, Boyle D, McArt D, et al. Molecular classification of non-invasive breast lesions for personalised therapy and chemoprevention. *Oncotarget*. 2015;6(41):43244-43254.
46. Aguiar FN, Cirqueira CS, Bacchi CE, Carvalho FM. Morphologic, molecular, and microenvironment factors associated with stromal invasion in breast ductal carcinoma in situ: role of myoepithelial cells. *Breast Dis*. 2015;35(4):249-252.
47. Aguiar FN, Mendes HN, Bacchi CE, Carvalho FM. Comparison of nuclear grade and immunohistochemical features in situ and invasive components of ductal carcinoma of breast. *Revista Brasileira de Ginecologia e Obstetrícia*. 2013;35(3):97-102.
48. Tsujikawa T, Kumar S, Borkar RN, et al. Quantitative multiplex immunohistochemistry reveals myeloid-inflamed tumor-immune complexity associated with poor prognosis. *Cell Rep*. 2017;19(1):203-217.
49. Schindelin J, Arganda-Carreras I, Frise E, et al. Fiji: an open-source platform for biological-image analysis. *Nat Methods*. 2012;9(7):676-682.
50. Carpenter AE, Jones TR, Lamprecht MR, et al. CellProfiler: image analysis software for identifying and quantifying cell phenotypes. *Genome Biol*. 2006;7(10):R100.
51. Chang YH, Guillaume T, Owen M, et al. Deep learning based nucleus classification in pancreas histological images. *Conf Proc IEEE Eng Med Biol Soc* 2017. 2017:672-675. <https://doi.org/10.1109/EMBC.2017.8036914>
52. Gray E, Mitchell E, Jindal S, Schedin P, Chang YH. A method for quantification of calponin expression in myoepithelial cells in immunohistochemical images of ductal carcinoma in situ. Paper presented at: 2018 IEEE 15th International Symposium on Biomedical Imaging (ISBI 2018); 4-7, 2018.
53. Sopik V, Sun P, Narod SA. Impact of microinvasion on breast cancer mortality in women with ductal carcinoma in situ. *Breast Cancer Res Treat*. 2018;167(3):787-795. <https://doi.org/10.1007/s10549-017-4572-2>
54. Marie B, Marie-Melanie D, Fabrice K, et al. Analysis of tumour-infiltrating lymphocytes reveals two new biologically different subgroups of breast ductal carcinoma in situ. *BMC Cancer*. 2018;18(1):129. <https://doi.org/10.1186/s12885-018-4013-6>
55. Xiao-Yang C, Joe Y, Aye Aye T, Boon Huat B, Puay Hoon T. Prognostic role of immune infiltrates in breast ductal carcinoma in situ. *Breast Cancer Res Treat*. 2019;173:1-11.
56. Campbell MJ, Baehner F, O'Meara T, et al. Characterizing the immune microenvironment in high-risk ductal carcinoma in situ of the breast. *Breast Cancer Res Treat*. 2016;161(1):17-28.
57. Sharpe AH, Pauken KE. The diverse functions of the PD1 inhibitory pathway. *Nat Rev Immunol*. 2017;18(3):153-167.
58. Toussaint J, Durbecq V, Rouas G, et al. CD10 expression and risk of relapse in DCIS. PMID-27963235. *J Clin Oncol*. 2009;27(15_suppl):e22053.
59. Sirka OK, Shamir ER, Ewald AJ. Myoepithelial cells are a dynamic barrier to epithelial dissemination. *J Cell Biol*. 2018;217(10):3368-3381.
60. Tian B, Ding X, Song Y, et al. Matrix stiffness regulates SMC functions via TGF- β signaling pathway. *Biomaterials*. 2019;221:119407.
61. Sameni M, Cavallo-Medved D, Franco OE, et al. Pathomimetic avatars reveal divergent roles of microenvironment in invasive transition of ductal carcinoma in situ. *Breast Cancer Research: BCR*. 2017;19(1):56.
62. Ding L, Su Y, Fassl A, et al. Perturbed myoepithelial cell differentiation in BRCA mutation carriers and in ductal carcinoma in situ. *Nat Commun*. 2019;10(1):4182.
63. Kim A, Heo S-H, Kim Y-A, Gong G, Lee HJ. An examination of the local cellular immune response to examples of both ductal carcinoma in situ (DCIS) of the breast and DCIS with microinvasion, with emphasis on tertiary lymphoid structures and tumor infiltrating lymphocytes. *Am J Clin Path*. 2016;146(1):137-144.
64. Hendry S, Pang JMB, Byrne DJ, et al. Relationship of the breast ductal carcinoma in situ immune microenvironment with clinicopathological and genetic features. *Clin Cancer Res*. 2017;23(17):5210-5217.
65. Schietinger A, Philip M, Krisnawan VE, et al. Tumor-specific t cell dysfunction is a dynamic antigen-driven differentiation program initiated early during tumorigenesis. *Immunity*. 2016;45(2):389-401.
66. Wang K, Li W, Yu Q, et al. High mobility group box 1 mediates interferon- γ -induced phenotypic modulation of vascular smooth muscle cells. *J Cell Biochem*. 2017;118(3):518-529.
67. Hansson GK. Interferon gamma inhibits both proliferation and expression of differentiation-specific alpha-smooth muscle actin in arterial smooth muscle cells. *J Exp Med*. 1989;170(5):1595-1608.
68. Guo Q, Minnier J, Burchard J, Chiotti K, Spellman P, Schedin P. Physiologically activated mammary fibroblasts promote postpartum mammary cancer. *JCI Insight*. 2017;2(6).

SUPPORTING INFORMATION

Additional supporting information may be found online in the Supporting Information section.

How to cite this article: Mitchell E, Jindal S, Chan T, et al. Loss of myoepithelial calponin-1 characterizes high-risk ductal carcinoma in situ cases, which are further stratified by T cell composition. *Molecular Carcinogenesis*. 2020;59:701-712. <https://doi.org/10.1002/mc.23171>